In Situ pH Monitoring in Turbid Coastal Waters Based on Self-Electrodeposition Ir/IrO2 Electrode

Article *in* Journal of The Electrochemical Society · August 2021

DOI: 10.1149/1945-7111/ac208b

6 authors, including:

Zhengwen Zhou
Ocean University of China
3 PUBLICATIONS **3** CITATIONS
SEE PROFILE

Dawei Pan
Chinese Academy of Sciences
58 PUBLICATIONS **608** CITATIONS
SEE PROFILE

Journal of The Electrochemical Society, 2021 **168** 097501

In Situ pH Monitoring in Turbid Coastal Waters Based on Self-Electrodeposition Ir/IrO_2 Electrode

Zhengwen Zhou,[1,2] Dawei Pan,[1,2,3,z] Chenchen Wang,[1,3] Haitao Han,[1,3] Hong Wei,[1,2] and Fei Pan[1,2]

[1]*CAS Key Laboratory of Coastal Environmental Processes and Ecological Remediation, Shandong Key Laboratory of Coastal Environmental Processes, Research Center for Coastal Environment Engineering Technology of Shandong Province, Yantai Institute of Coastal Zone Research, Chinese Academy of Sciences, Yantai 264003, People's Republic of China*
[2]*University of Chinese Academy of Sciences, Beijing 100049, People's Republic of China*
[3]*Center for Ocean Mega-Science, Chinese Academy of Sciences, Qingdao 266071, People's Republic of China*

Direct and accurate monitoring of pH in turbid waters is a challenging task for environmental monitoring and analysis. In this study, iridium oxide (IrO_2) with selective sensing ability toward H^+ was produced on the surface of iridium (Ir) electrode by rapid self-electrodeposition. IrO_2 was deposited on electrode surface by atomic force, which could decrease the adverse effect of the suspended particles in turbid water. Properties of the Ir/IrO_2 electrode were investigated by X-ray photoelectron spectroscopy, scanning electron microscopy, and electrochemical technology. The sensitivity and response time of the Ir/IrO_2 electrode for pH determination were assessed, and a rapid and linear pH response of approximately 65 ± 3.5 mV pH^{-1} was observed across a wide pH range between 1.8 and 11.9. Moreover, the electrode exhibited a good temperature linearity (20 °C–60 °C), low potential drift (0.75 mV h^{-1}), high accuracy (±0.05), and a long life span (up to 30 d). The practical investigation revealed faster equilibrium rate and higher stability of the Ir/IrO_2 electrode than that of traditional glass pH electrode. Furthermore, the Ir/IrO_2 electrode was successfully used for in situ pH monitoring in 750 formazin turbidity units (FTU) for turbid coastal river water. Therefore, the developed Ir/IrO_2 pH electrode offers large applicability for in situ pH monitoring in turbid environmental water matrices.
 [DOI: 10.1149/1945-7111/ac208b]

Manuscript submitted January 29, 2021; revised manuscript received August 10, 2021. Published September 2, 2021.

Supplementary material for this article is available online

pH is an important environmental parameter, which significantly affects many environmental factors including water quality,[1] ecosystem health,[2] and geochemical processes.[3] Turbid water contains numerous suspended particles, which are capable of absorbing various pollutants, heavy metals, and nutrients. In particular, the heavy metal adsorption and desorption process is affected by pH fluctuations in water.[4,5] With the intensification of ocean acidification, pH levels in high-turbidity coastal estuaries and ocean areas may get affected, leading to desorption of heavy metals adsorbed on suspended particles.[6–9] Therefore, in situ pH monitoring in turbid waters is useful for exploring the migration and transformation of heavy metals in geochemical processes.

At present, pH in natural water matrices is mainly determined by two principal methodologies, namely, the electrochemical method using a potentiometer and the spectral method using pH-sensitive colorimetric indicator dyes.[10] For the electrochemical method, traditional pH electrodes with glass membranes have been most frequently reported. These electrodes are used extensively owing to their simple structure and convenient method of mass production.[11,12] However, these mechanically fragile electrodes can be damaged to some extent by erosion due to suspended sediments in estuarine zones.[13,14] The spectrophotometric method has limited use for monitoring pH in high-turbidity estuary areas, as the transmission light is affected by sediments and suspended particulate matter, increasing the deviation of results.[15] Therefore, development of some new technologies and methods to effectively achieve in situ pH monitoring of complex turbid water is a challenging task.

Recently, solid metal oxide pH electrodes have attracted significant research attention owing to their excellent resistance to high pressure and extreme environments.[16] Solid metal oxide electrodes measure pH using electron transfer between metals/metal oxides and the exchange of H^+ ions in the metal oxide/aqueous solution.[17] Therefore, the concentration of H^+ ions in aqueous solution can be determined by correlation (conforming to the Nernst equation) between the electric potential difference at the interface and the pH of the solution.[17,18] Among the assessed solid metal-oxide electrodes, iridium oxide (IrO_x) pH electrodes have been proven to exhibit a rapid and sensitive response to pH over a broad range.[19] The principal literature methods of preparation of iridium oxide pH electrodes include electrodeposition,[20] heat-treatment,[21,22] sputtering deposition,[23] and electrochemical growth.[24] There are also several in-depth reviews and reports summarizing the methods developed for the fabrication of iridium oxide electrodes and their application for environmental monitoring and living organism analysis.[25–29]

The electrodeposition method involves placement of the substrate in an iridium salt solution for electrodeposition. However, the iridium oxide film deposited by the iridium salt easily detaches with long-term application. In contrast, both the heat-treatment and sputtering deposition procedures require extreme preparation conditions, with high temperatures above 400 °C,[30,31] making it difficult to use these processes under conventional laboratory conditions.

Among the above-mentioned methods for preparing iridium electrode, the traditional electrodeposition method requires complex deposition solution with strict ratio.[32,33] Thermal oxidation and thermal sputtering require high-temperature oxidation instruments,[34,35] which are generally expensive, further limiting the application of iridium-based electrodes. In this study, the bulk iridium electrode using simple self-electrodeposition approach was prepared by cyclic voltammetry (CV) technology, which has the advantages of cost effectiveness, simple preparation, and good response performance.

In this study, iridium oxide particles were produced on the surface of Ir wire by easy self-electrodeposition. The iridium oxide particles firmly deposited on the Ir substrate by atomic force, which reduced the erosion of the surface film by suspended particles, thus improving the electrode sensing performance. The experimental parameters and performance of the Ir/IrO_2 electrode in turbid coastal river water were tested systematically. Finally, the practical

[z]E-mail: dwpan@yic.ac.cn

application of the Ir/IrO_2 electrode for in situ pH determination was assessed in real coastal water samples.

Materials and Methods

Materials and instruments.—Electrochemical experiments including CV and open circuit potential (OCP)-time trace were performed using a CHI660E electrochemical workstation and 1230C Palmtop Potentiostat (ChenHua, Shanghai, China). Morphologies of the pristine and fabricated electrodes were characterized by scanning electron microscopy (SEM, Hitachi S-4800 microscope, Japan) and X-ray spectroscopy (XPS, Thermo ESCALAB 250XI, US). A series of pH buffer solutions was determined and calibrated using an E-201-C pH meter (INESA, Shanghai, China), for measuring the pH in estuaries zones using the Ir/IrO_2 pH electrode, and then the results were compared with measurements carried out using a portable PHB-4 pH meter (INESA, Shanghai, China). Temperature control tests were performed using a super constant temperature water-bath (HH-601, Changzhou, China). The modified solid Ir electrode served as the working electrode, with Ag/AgCl (3.0 M KCl) and platinum foil serving as the reference and counter electrodes, respectively. All potentials were measured with respect to the Ag/AgCl reference electrode.

Pure Ir wire (99.9%, 0.25 mm in diameter) was purchased from Sino-Precious Metals Holding Co., Ltd. (Kunming, China). Potassium hydroxide (KOH), ethanol (CH_3CH_2OH), and hydrochloric acid (HCl) were purchased from Sinopharm Chemical Reagent Co., Ltd. (Shanghai, China). Standard pH buffer solutions at pH 4.00 (potassium hydrogen phthalate), 6.86 (mixed phosphate), and 9.18 (borax) were purchased from INESA Scientific Instrument Co., Ltd. (Shanghai, China). Deionized water obtained using a Pall Cascada laboratory water system (Cascade-Bio, US) was used throughout. All chemicals were of analytical reagent grade and used without further purification. A series of phosphoric buffer solutions (PBS) in pH range from 1.83 to 11.97 was prepared using the phosphoric acid and phosphate system.

Preparation of the solid Ir/IrO_2 electrode.—First, Ir wire was polished with fine sandpaper to remove surface impurities. Then, sections of Ir wire with approximately 2 cm in length were ultrasonically cleaned in alternate solutions of 3 M HCl for 5 min and de-ionized water for 20 min. Subsequently, Ir wire was placed in potassium hydroxide solution, applying CV scanning from 0 to 0.7 V at a rate of 50 mV s^{-1}.[36] Under these conditions, the solid Ir/IrO_2 electrode was fabricated by self-electrodeposition. Finally, the fabricated Ir/IrO_2 electrode was rinsed with deionized water and immersed in 0.1 M HCl solution for at least 8 h to ensure hydrogen ions occupied the binding sites of the electrode to a maximum level.

Preparation of water samples.—Coastal river water and coastal seawater were collected from the Yellow River Estuary, China (Fig. S1 available online at stacks.iop.org/JES/168/097501/mmedia of the Supporting Information). The samples were collected and stored in polyethylene bottles at 4 °C during transport to the laboratory, then maintained under these conditions prior to performing short-term stability and turbidity tests using the fabricated Ir/IrO_2 electrodes.

Optimization of preparation conditions.—The Ir/IrO_2 electrodes were prepared in potassium hydroxide solution (pH 11.0, 12.0, or 13.0) with different cycles (5, 10, 20, 30, or 40). PBS solutions with pH in the range 1.8–11.9 were used to test the electrode. Moreover, potential was measured by recording OCP against an Ag/AgCl reference electrode. The response slope and linear correlation coefficient R^2 of the electrode were obtained.

Performance testing procedure.—The electrodes were connected to the workstation, and the temperature was controlled using a water bath. The potential value of the electrode was measured in various phosphoric buffer solutions (pH 1.8–11.9) at different temperatures ranging from 20 to 60 °C, to evaluate the effects of pH and temperature on the electrode potential. For the stability test, the electrodes were immersed in the collected coastal seawater samples, and the electrochemical parameters were set as follows: OCP limit of 0.1 to 0.5 V, sample interval of 0.1 s, and run time of 30000 s. For long-term life-span measurements, the electrodes were immersed in PBS for 30 d, with deionized water supplemented from time to time to account for evaporation.

Electrochemical analysis procedure.—The prepared Ir/IrO_2 electrode was first immersed in deionized water for 2 h to promote ion balance on the surface of the electrode and obtain a stable OCP. Then, the working electrode was calibrated in the standard buffer solutions of pH 4.00, 6.86, and 9.18 to obtain an electrode calibration curve. The calibrated parameter slope and potential $E^{0'}$ (reference in formula 2) were uploaded to the sensor storage system. The calibration curve was utilized for pH detection in turbid waters, and the pH of the turbid waters was established based on the measured potential value.

Results and Discussion

The self-electrodeposition method in this study utilizes a redox reaction between the Ir wire and hydroxyl ions in a strongly alkaline solution by electrochemical technology, with iridium oxide, an H^+ selective material, formed on the surface of the Ir wire. Figure S2 shows a schematic illustration of the basic self-electrodeposition process, which is similar to the related reported processes for iridium oxide preparation.[37–39] Compared to the self-electrodeposition process in alkaline solution, no oxidation phenomenon was observed from the CV curves of the Ir electrode under various concentrations of HCl (Fig. S3).

Sensing mechanism.—A schematic illustration of the electrode preparation and monitoring mechanism is illustrated in Fig. 1. Surface components of the Ir wire lose electrons to produce IrO_2 through a redox reaction with OH^- ions in alkaline solution. The specific reaction formula for generating IrO_2 is specified in Eq. 1:

$$Ir - 4e^- + 4OH^- \rightarrow IrO_2 + H_2O \quad [1]$$

The results of the pH sensor system correspond to the potential difference between the working electrode and the Ag/AgCl reference electrode.[40–42] As a metal oxide system, the potential reaction mechanism between the Ir/IrO_2 electrode and hydrogen ions is shown in Eq. 2:[17]

$$2IrO_2 + 2H^+ + 2e^- \leftrightarrow Ir_2O_3 + H_2O \quad [2]$$

$$E = E^0 + \frac{2.303RT}{2F} \cdot log \frac{IrO_2{}^2}{Ir_2O_3} + \frac{2.303RT}{nF} log[H^+]$$

$$E^{0'} = E^0 + \frac{2.303RT}{2F} \cdot log \frac{[IrO_2^2]}{[Ir_2O_3]}$$

$$E = E^{0'} - \frac{2.303RT}{nF} pH$$

where E^0 is the standard redox potential of the electrode, E is the measured potential (V), F is the Faraday's constant with a value of 23062 cal.V^{-1} or 96406 J.V^{-1}, R is the gas constant (8.314 J.K^{-1}.mol^{-1}), T is the absolute temperature (K), and n is the number of electrons transferred per proton in the redox reaction. The stability of $E^{0'}$ depends on the ratio of Ir(III) and Ir(IV), which is related to the oxidation state of the surface of the electrode.

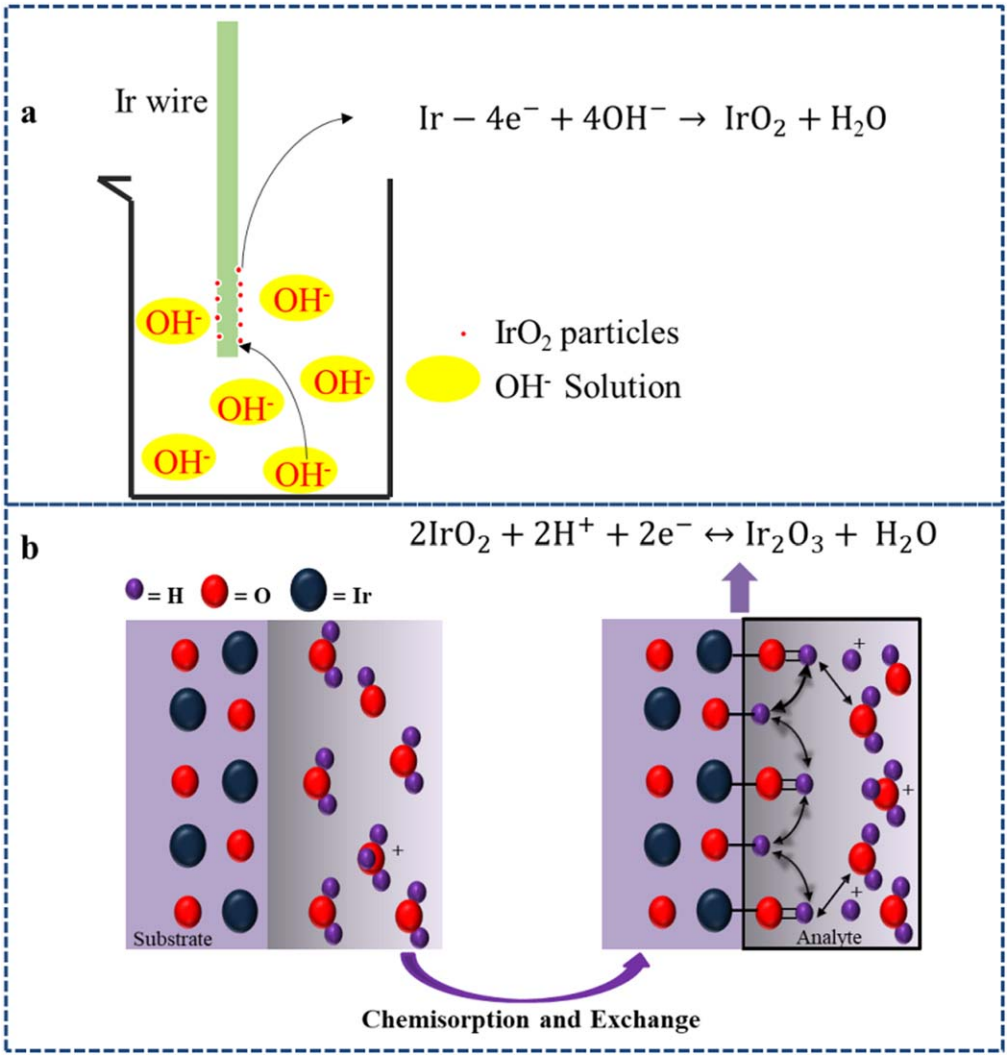

Figure 1. (a) Self-electrodeposition mechanism of the Ir/IrO_2 electrode and (b) the mechanism of pH determination using the Ir/IrO_2 electrode.

Characterization of the Ir/IrO$_2$ electrode.—The surface composition of the Ir wire electrode in its pristine form and after self-electrodeposition was analyzed by XPS, and the Ir 4 f and O 1 s spectra and their deconvolutions is illustrated in Fig. 2. According to literature, the binding energies (BEs) of Ir^{4+} are 61.7 eV (4 f 7/2) and 64.9 eV (4 f 5/2).[43,44] Therefore, the appearance of BEs at 61.8 eV 4 f (7/2) and 64.8 eV 4 f (5/2) indicates the presence of Ir^{4+} in this present study. Furthermore, a comparative analysis of Figs. 2a and 2b indicates that the ratio of Ir^0 to Ir^{4+} increased from 0.40 to 0.48, revealing that the ratio of Ir^{4+} increased as a result of self-electrodeposition. The O 1 s spectrum of the Ir wire before self-electrodeposition could be deconvoluted into three peaks at 530.5, 531.8, and 533.3 eV, attributing to IrO_2, OH^-, and C=O, respectively. The ratio of IrO_2 content before and after the self-electrodeposition process increased from 6.9 to 32.4%. Figure 2d demonstrates that the observed shifts of BE were possibly because of more oxide ions being bound to Ir^{4+} during the oxidation process.

Ir/IrO_2 electrode sensing depends on the oxide layer on the electrode surface, as IrO_2 is directly generated on the surface of Ir wire using electrochemical technology. The micromorphology of the surfaces of the pristine electrode and the Ir/IrO_2 electrode is presented in Fig. 3, showing that the electrochemically grown electrode surface was covered with a layer of particles, with the diameter ranging between 50–300 nm.

Optimization of electrode performance.—The response slope and correlation coefficient (R^2) of the pH electrode are two important parameters, with the response slope representing the sensitivity of the electrode, where higher sensitivity results in the electrode reaching equilibrium in a shorter period.

Figure 4a exhibits the response slope of the Ir/IrO_2 electrode under different self-electrodeposition cycles, with the error bar referring to the slope error of the electrode under the same scan cycles. The results show that the response slope of the series of Ir/IrO_2 pH electrodes ranged from –51.5 to –69.1 mV pH^{-1}. The response slope of the electrode obviously increased from 50.8 to 66.0 mV pH^{-1} with increasing CV cycles from 5 to 20, while the relative standard deviation (RSD) of slope tended to decrease accordingly. Furthermore, the average response slope of the Ir/IrO_2 pH electrode decreased from 66.0 to 61.0 mV pH^{-1}, and the slope RSD slowly increased with increasing electrodeposition cycles from 20 to 40. The phenomenon of initial increase in response of slope is likely because of increasing content of iridium oxide on the surface of the electrode with an increased number of self-electrodeposition cycles. The increase in the number of iridium oxide particles can hinder the proton transport, decreasing the response slope of the electrode.

Furthermore, the correlation coefficient R^2 of the electrode was also affected by different pH conditions and the number of self-electrodeposition cycles. Figure 4b illustrates that the stability of the electrode was influenced by OH^- under different alkaline

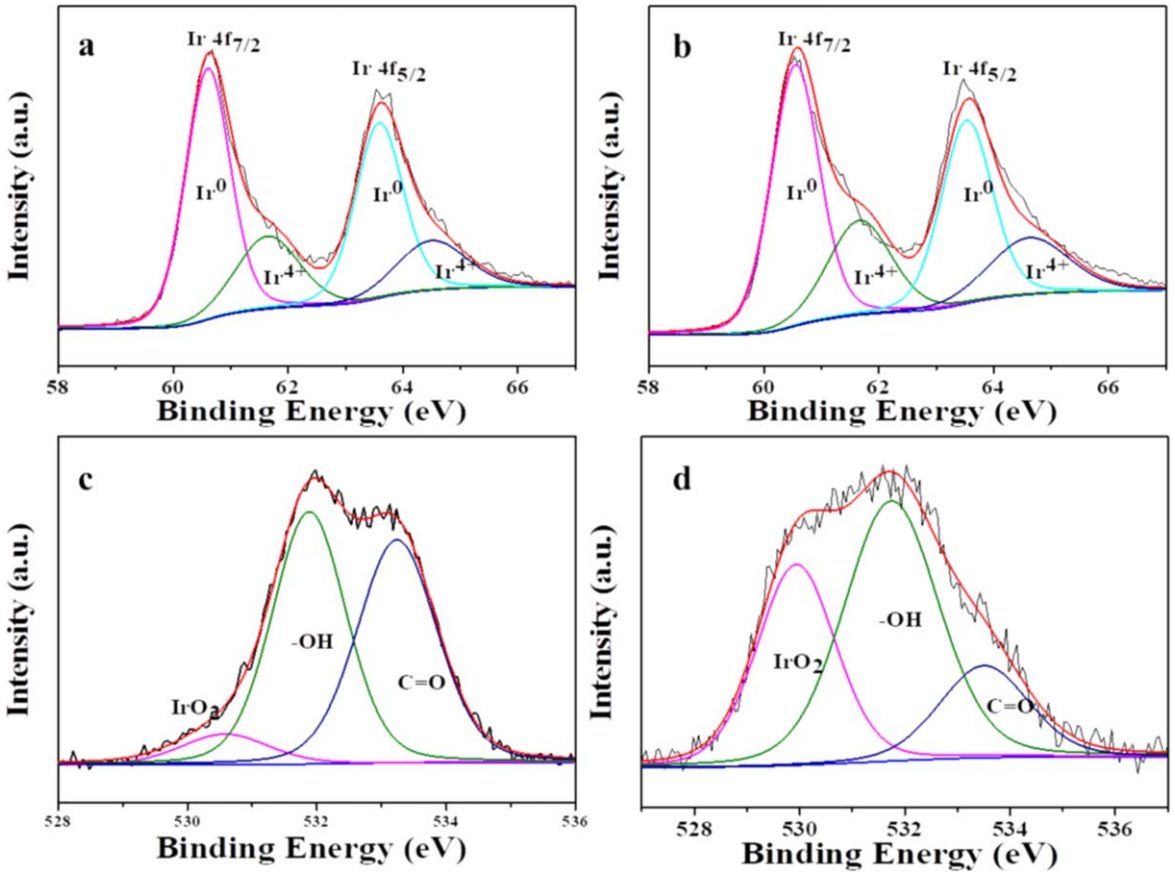

Figure 2. XPS spectra of the bare iridium wire electrode: (a) Ir 4 f spectra and (c) O 1 s spectra; XPS spectra of the Ir/IrO_2 electrodes: (b) Ir 4 f spectra and (d) O 1 s spectra.

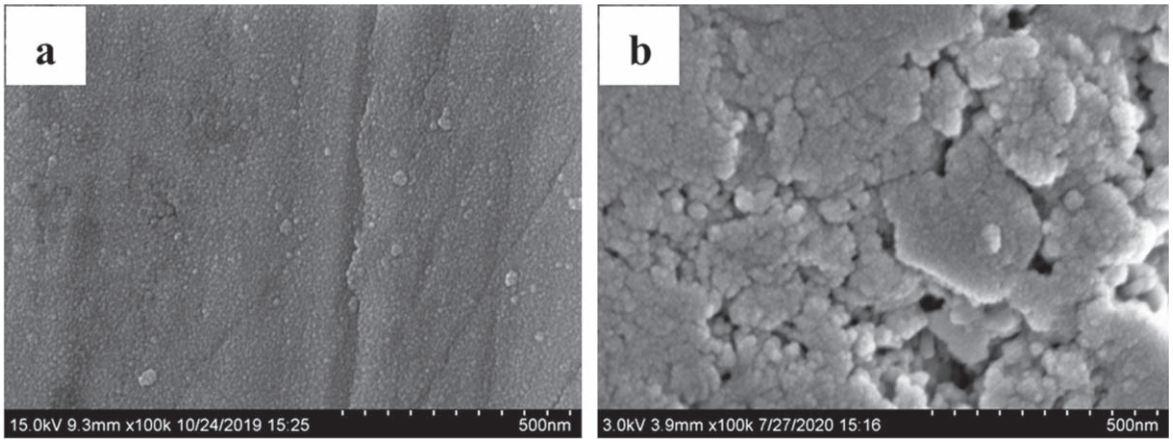

Figure 3. Typical SEM images of the surface of (a) bare iridium wire and (b) self-electrodeposited IrO_2 particles on the Ir electrode surface.

conditions. Compared to the condition of hydrogen ion concentration, the electrode made under strong alkaline conditions (pH = 13) exhibited a higher scanning correlation from 5 to 40 cycles, with a maximum R^2 value observed for 20 scanning cycles. Therefore, the Ir/IrO_2 pH electrode exhibited optimal performance when prepared using the self-electrodeposition method under alkaline conditions (pH = 13) with 20 cycles of deposition.

Performance tests.—In order to investigate the effects of temperature change on electrode performance, a series of temperature tests was performed. The results exhibited that the Ir/IrO_2 electrode maintained good linearity in the range 20 °C–60 °C, producing a non-significant change (from −53.31 mV pH^{-1} at 20 °C to −52.54 mV pH^{-1} at 40 °C) in the electrode calibration curve in the range 20 °C–40 °C (Fig. 5a). Therefore, the Ir/IrO_2 electrode can be used for measurements within a narrow temperature range, with a small deviation in results, which could simplify temperature calibration procedures in practical applications.

Subsequently, the stability of the Ir/IrO_2 electrode under short- and long-term conditions was studied. Figure 5b shows that the short-term stability of the Ir/IrO_2 electrode indicated that the potential of the electrode exhibited a 4 mV shift when placed in surface coastal seawater medium for 8 h. Coastal seawater is a complex substrate, containing a large amount of Na^+. It has been

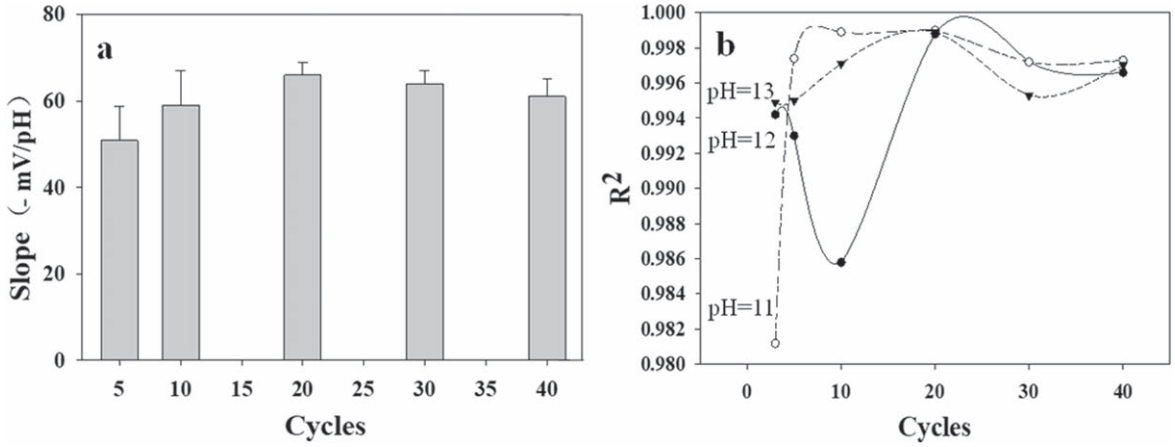

Figure 4. (a) The relationship between the Ir/IrO_2 pH electrode response slope and the number of self-electrodeposition cycles and (b) curve of the number of self-electrodeposition cycles with the electrode correlation coefficient (R^2) under different pH conditions.

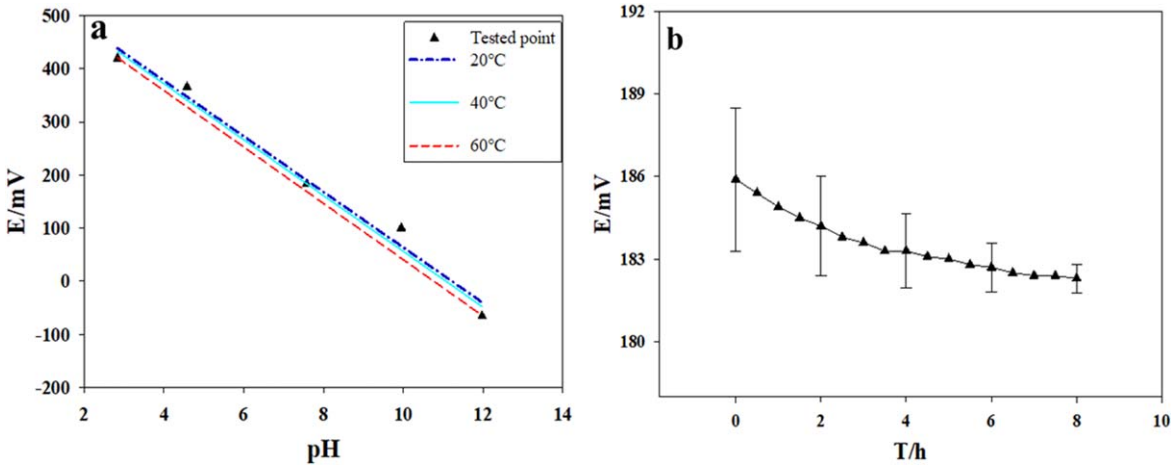

Figure 5. (a) Simulation test results at temperatures ranging from 20 °C–60 °C and (b) Stability test results of Ir/IrO_2 pH electrodes in coastal seawater for 8 h (n = 3).

previously reported that potential drift is promoted by the existence of Na^+, which is referred as the alkali error.[45,46] The standard deviations of metal oxide pH electrodes have previously been reported for RuO_2-Ta_2O_5,[47] IrO_2/Pt,[23] and iridium oxide film[21] pH electrodes, exhibiting errors of approximately ±0.15, ±0.10, and ±0.04 pH, respectively. In this study, monitoring for 8 h showed electrode deviation of about ±0.05 pH, within an acceptable range (drift 0.75 mV h^{-1}). The long-term response of the Ir/IrO_2 electrode is shown in Fig. 6, indicating that the electrode maintained a good linear response after 30 d. However, the response slope of the electrode decreased with increasing placement time, which might have potentially resulted from a reduction in IrO_2 particles.

Components and characteristics of the sensor.—The accuracy of the electrode was evaluated (Table SI) by comparing the deviation in standard buffer solutions, illustrating that the Ir/IrO_2 pH electrode exhibited good accuracy. Figure S4a illustrates the four main components of the sensor, including working electrode, reference electrode, temperature calibration sensor, and microcontrollers. Figure S4b shows diagram of the pH meter calibration system used for the measurement. The slope K and $E^{0'}$ values of the initial response curve of the detector were obtained using two different buffer solutions. Then, according to the difference between the measured solution temperature and room temperature, it was decided whether to carry out the temperature calibration or not. When the difference was rather large (over the range 20 °C–40 °C), temperature calibration was carried out in the same standard buffer solution with two temperature differences to obtain the temperature calibration coefficient K_T. The potential value of the solution is described in Eq. 3:

$$E_x = E^{0'} - KpH_x - K_T(T_x - T_0) \quad [3]$$

where pH_x, E_x, and T_x are the pH, potential, and temperature value of solution to be tested, respectively. T_0 is the temperature of standard buffer solution.

Owing to the increased program control steps, the sensor data output showed a hysteresis phenomenon. Specifically, the detector has 20 data points with an interval of 10 s and a hysteresis of about 200 s.

In situ analysis and application.—Figure 7a exhibits the determined result of turbid water of the Yellow River using two different types of glass electrodes and the solid-state Ir/IrO_2 electrode. Compared to the two glass electrodes (PHB-4 pH meter and E-201-C pH meter), the equilibrium time of the solid-state Ir/IrO_2 electrode was less than 3 min, which is significantly lower than that of the portable glass pH electrode. Moreover, the fluctuation of pH measured using the electrode was relatively small, confirming high measurement stability of the electrode used in this study. Figure 7b shows the reproducibility of the electrode. The electrode was used in the turbid water for one determination each

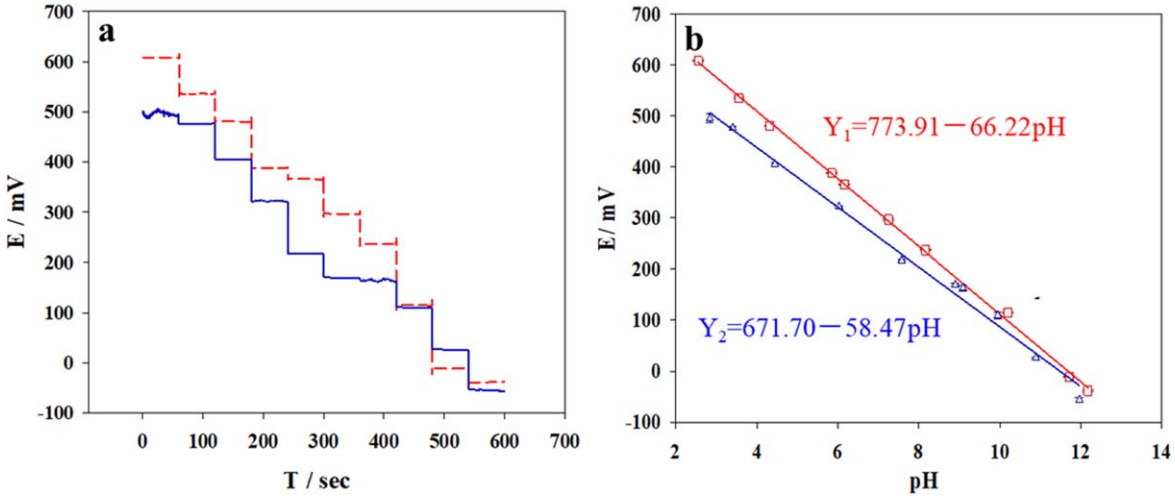

Figure 6. Long-term life span evaluation of the Ir/IrO_2 pH electrode in phosphoric acid buffer solution: (a) potential change and (b) calibration slope. Red indicates the 2nd day after electrodes preparation, blue indicates 30 d after electrodes preparation.

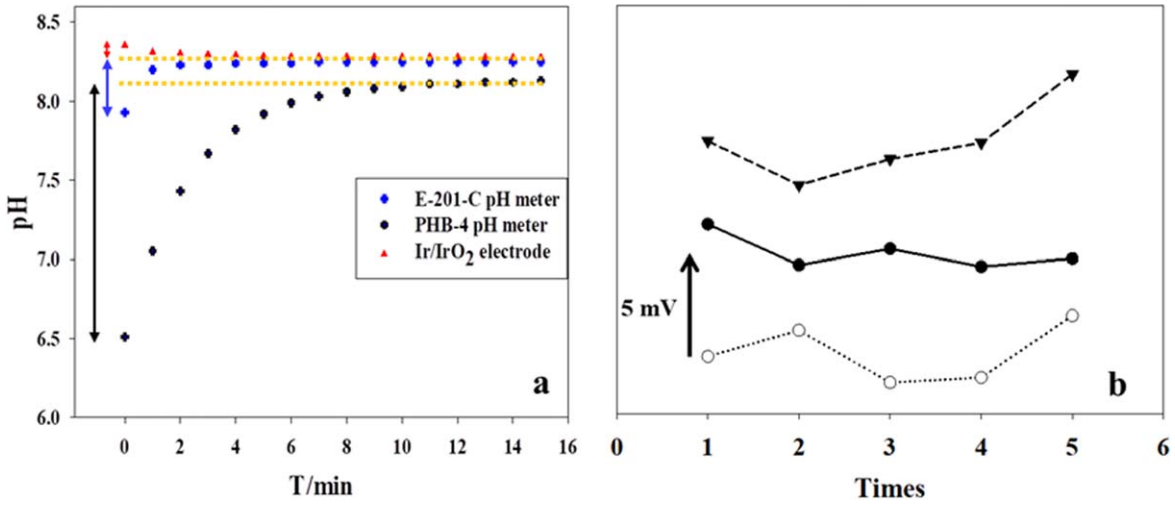

Figure 7. (a) Comparison of stability and response rate between the Ir/IrO_2 pH electrode and glass pH electrodes in turbid water and (b) Continuous measurement using the three Ir/IrO_2 pH electrodes for five times.

day. The results showed that the RSD of the electrodes was in the range 1.1%–2.5%.

The sensor was then taken to the Yellow River Estuary to carry out the test on turbid coastal river water (Table SII). When high-turbidity Yellow River water was tested in situ in the estuary environment, which is affected by both the river water and seawater flow, pH fluctuation was observed at the determination site. Figure 8 illustrates that the variation in ambient pH was measured online for 1 h in situ, with the sensor measurements in the Yellow River estuary fluctuating between 8.0 and 8.15. At the same time, the Ir/IrO_2 pH electrode exhibited a rapid response and good stability in 750 formazin turbidity units (FTU) turbid water (ranging from 7.1 to 9.1), with pH fluctuation caused by surrounding environmental conditions. Table I shows the comparison of the Ir/IrO_2 pH electrode with other electrodes developed for pH determination, indicating that compared to other electrodes and their corresponding applications, the Ir/IrO_2 pH electrode exhibited superior performance for pH determination in turbid coastal river water. Therefore, these findings verify that the Ir/IrO_2 electrode performed well for in situ determination of pH in highly turbid waters.

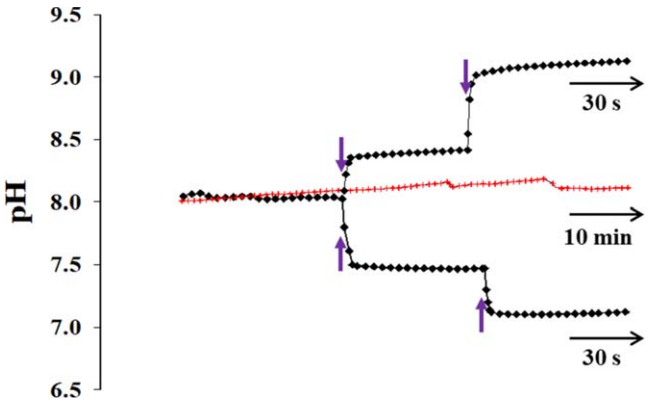

Figure 8. In situ pH monitoring in turbid coastal river water using the Ir/IrO_2 pH electrode (red line) and pH response test in coastal river water (black line).

Conclusions

This study provides a novel methodology for monitoring pH of high-turbidity water using a solid-state Ir/IrO_2 electrode. The self-

Table I. Comparison of characteristics and performance of the Ir/IrO_2 electrode with other reported electrode substrates.

Substrates type	Surface structure	Fabrication method	Sensitivity (mV/pH)	Measurement range	Response Time (s)	Drift (mV/h)	Application	References
IrO_2/Pt	Ta_2O_5	Sputtering	−59.5	2–13	—	<0.5	Water solution	Kuo et al.[23]
Indium tin oxide	Iridium oxide nanowires	Electrodeposits	−90.1	0–13	Within 30	—	Human skin sweat	Zhou et al.[33]
Gold-foil	Iridium oxide films	Thermal oxidization	near −59.2	2–10	—	0.12	Water solution	Sun et al.[34]
ITO/PET	PDDA/IrO_x polymer layers	Alternate deposition	average −58.4	2.91–10.37	2–3	1.56	Biomedical, clinical analysis	Jovic et al.[48]
Pt electrode	Iridium oxide films	Electrodeposition	−67.60	2.22–11.81	less than 7	0.31	Water quality	Zhou et al.[49]
Gold microneedles	IrO_x films	Electrodeposition	−75.39 ± 0.07	4–8	40	9	Biochemical analysis	Cork et al.[50]
Iridium microdisc	Iridium oxide films	Electrodeposition	−56.3 to −69.4	2–8	—	—	Blood	Chaisiwamongkhol et al.[51]
Iridium wires	Iridium oxide layer	Thermal oxidation	−57.1	2–12	About 30	12	Distilled water	Ratanaporncharoen et al.[52]
Iridium wire	Surface IrO_2 particles	CV electrodeposition	−65 ± 3.5	1.8–11.9	10	0.75	Turbid water	This study

electrodeposition process resulted in the formation of iridium particles on the electrode surface, endowing the Ir/IrO_2 electrode with the ability to resist erosion. The Ir/IrO_2 pH electrode demonstrated a rapid response under fluctuating pH conditions, with excellent sensitivity, long lifetime, and stability under a broad pH range from 1.8 to 11.9. Furthermore, the Ir/IrO_2 electrode was successfully used for in situ monitoring of pH changes in turbid coastal river water.

Acknowledgments

This study was financially supported by the Original Innovation Project of Chinese Academy of Sciences (ZDBS-LY-DQC009), the Strategic Priority Research Program of Chinese Academy of Sciences (XDB42000000), the National Key R&D Program of China (2019YFD0901103).

Data availability statement

N.A

ORCID

Zhengwen Zhou https://orcid.org/0000-0002-5213-5287
Dawei Pan https://orcid.org/0000-0002-6166-9707
Haitao Han https://orcid.org/0000-0002-5389-6256

References

1. Y. Lu, X. Gao, and C.-T. A. Chen, *Mar. Chem.*, **215**, 103685 (2019).
2. B. Cancino-Madariaga, C. F. Hurtado, and R. Ruby, *Aquac. Eng.*, **45**, 103 (2011).
3. M. V. Ardelan and E. Steinnes, *Biogeosciences*, **7**, 569 (2010).
4. V. Hatje, T. E. Payne, D. M. Hill, G. McOrist, G. F. Birch, and R. Szymczak, *Environ. Int.*, **29**, 619 (2003).
5. A. R. Wilson, L. W. Lion, Y. M. Nelson, M. L. Shuler, and W. C. Ghiorse, *Environ. Sci. Technol.*, **35**, 3182 (2001).
6. Y. W. Watanabe, B. F. Li, and M. Wakita, *Geophys. Res. Lett.*, **45**, 9106 (2018).
7. X. Zeng, X. Chen, and J. Zhuang, *Mar. Pollut. Bull.*, **91**, 14 (2015).
8. Q. Yao, X. Wang, H. Jian, H. Chen, and Z. Yu, *Int. J. Environ. Res. Public Health*, **12**, 6725 (2015).
9. Z.-L. Wang and C.-Q. Liu, *Chem. Geol.*, **202**, 383 (2003).
10. S. F. Gonski, W. J. Cai, W. J. Ullman, A. Joesoef, C. R. Main, D. T. Pettay, and T. R. Martz, *Estuar. Coast. Shelf Sci.*, **200**, 152 (2018).
11. J. C. Seiter and M. D. Degrandpre, *Talanta*, **54**, 99 (2001).
12. M. Wang and S. Yao, *Electroanalysis*, **15**, 1606 (2003).
13. M. Glanc-Gostkiewicz, M. Sophocleous, J. K. Atkinson, and E. Garcia-Breijo, *Sens Actuators A Phys.*, **202**, 2 (2013).
14. M. Luniak and K. J. Wolter, *3rd International Micro Materials Conference* (DDP Goldenbogen Sigurd, Dresden, Germany) (2000).
15. T. R. Martz, J. G. Connery, and K. S. Johnson, *Limnol. Oceanogr. Meth.*, **8**, 172 (2010).
16. P. J. Kinlen, J. E. Heider, and D. E. Hubbard, *Sens. Actuator B-Chem.*, **22**, 13 (1994).
17. R. H. G. Mingels, S. Kalsi, Y. Cheong, and H. Morgan, *Sens. Actuator B-Chem.*, **297**, 126779 (2019).
18. J. Yang, T. J. Kwak, X. D. Zhang, R. McClain, W. J. Chang, and S. Gunasekaran, *ACS Sens.*, **1**, 1235 (2016).
19. G. M. Da Silva, S. G. Lemos, L. A. Pocrifka, P. D. Marreto, A. V. Rosario, and E. C. Pereira, *Anal. Chim. Acta*, **616**, 36 (2008).
20. K. Yamanaka, *Jpn. J. Appl. Phys.*, **28**, 632 (1989).
21. Y. Pan, Z. Sun, H. He, Y. Li, L. You, and H. Zheng, *Sens. Actuator B-Chem.*, **261**, 316 (2018).
22. A. M. Zimer, M. Medina Da Silva, E. G. Machado, H. Varela, L. H. Mascaro, and E. C. Pereira, *Anal. Chim. Acta*, **897**, 17 (2015).
23. L. M. Kuo, Y.-C. Chou, K.-N. Chen, C.-C. Lu, and S. Chao, *Sens. Actuator B-Chem.*, **193**, 687 (2014).
24. E. E.-D. M. El-Giar and D. O. Wipf, *J. Electroanal. Chem.*, **609**, 147 (2007).
25. Z. Zhou, J. Li, D. Pan, H. Wei, C. Wang, F. Pan, J. Xia, and S. Ma, *Trends Environ. Anal. Chem.*, **25**, e00083 (2020).
26. H. Jang and J. Lee, *J. Energy Chem.*, **46**, 152 (2020).
27. W.-D. Huang, H. Cao, S. Deb, M. Chiao, and J. C. Chiao, *Sens Actuators A Phys.*, **169**, 1 (2011).
28. I. A. Ges, B. L. Ivanov, D. K. Schaffer, E. A. Lima, A. A. Werdich, and F. J. Baudenbacher, *Biosens. Bioelectron.*, **21**, 248 (2005).
29. S. A. M. Marzouk, S. Ufer, R. P. Buck, T. A. Johnson, L. A. Dunlap, and W. E. Cascio, *Anal. Chem.*, **70**, 5054 (1998).
30. Y. Ha and M. Wang, *Electroanalysis*, **18**, 1121 (2006).
31. F. Huang, Y. Jin, L. Wen, D. Mu, and M. Cui, *J. Electrochem. Soc.*, **160**, B184 (2013).
32. S. Carroll and R. P. Baldwin, *Anal. Chem.*, **82**, 878 (2010).
33. L. Zhou, C. Cheng, X. Li, J. Ding, Q. Liu, and B. Su, *Anal. Chem.*, **92**, 3844 (2020).
34. Z. Sun, Q. Ma, Y. Wang, and Y. Pan, *J. Electrochem. Soc.*, **167**, 047501 (2020).
35. D. Wang, C. Yang, J. Xia, Z. Xue, D. Jiang, G. Zhou, X. Zheng, H. Zheng, Y. Du, and Q. Li, *Ionics*, **23**, 2167 (2017).
36. X. Zhang, Y. Ye, Y. Kan, Y. Huang, J. Jia, Y. Zhao, C.-T. A. Chen, and H. Qin, *Acta Oceanol. Sin.*, **36**, 99 (2017).
37. P. Steegstra and E. Ahlberg, *Electrochim. Acta*, **68**, 206 (2012).
38. J. F. Rivera, I. Pignot-Paintrand, E. Pereira, B. L. Rivas, and J.-C. Moutet, *Electrochim. Acta*, **110**, 465 (2013).
39. H. Ooka, A. Yamaguchi, T. Takashima, K. Hashimoto, and R. Nakamura, *J. Phys. Chem. C*, **121**, 17873 (2017).
40. J. E. Baur and T. W. Spaine, *J. Electroanal. Chem.*, **443**, 208 (1998).
41. F. Huang, Y. Jin, L. Wen, and Z. Wan, *J. Electrochem. Soc.*, **165**, B12 (2018).
42. M. Khalil, S. Wang, J. Yu, R. L. Lee, and N. Liu, *J. Electrochem. Soc.*, **163**, B485 (2016).
43. M. Rubel, R. Haasch, P. Mrozek, A. Wieckowski, C. Depauli, and S. Trasatti, *Vacuum*, **45**, 423 (1994).
44. J. Riga, C. Tenretnoel, J. J. Pireaux, R. Caudano, J. J. Verbist, and Y. Gobillon, *Phys. Scr.*, **16**, 351 (1977).
45. S. Yao, M. Wang, and M. Madou, *J. Electrochem. Soc.*, **148**, H29 (2001).
46. C. C. M. Martinez, R. E. Madrid, and C. J. Felice, *IEEE Trans. Educ.*, **52**, 133 (2009).
47. L. Manjakkal, K. Zaraska, K. Cvejin, J. Kulawik, and D. Szwagierczak, *Talanta*, **147**, 233 (2016).
48. M. Jovic, J. C. Hidalgo-Acosta, A. Lesch, V. C. Bassetto, E. Smirnov, F. Cortes-Salazar, and H. H. Girault, *J. Electroanal. Chem.*, **819**, 384 (2018).
49. B. Zhou, C. Bian, J. Tong, and S. Xia, *Sensors*, **17**, 157 (2017).
50. S. C. Cork, A. Eftekhar, K. B. Mirza, C. Zuliani, K. Nikolic, J. V. Gardiner, S. R. Bloom, and C. Toumazou, *J. Neural Eng.*, **15**, 016001 (2018).
51. K. Chaisiwamongkhol, C. Batchelor-Mcauley, and R. G. Compton, *Analyst*, **144**, 1386 (2019).
52. C. Ratanaporncharoen, M. Tabata, N. Watanagool, T. Goda, A. Matsumoto, M. Sriyudthsak, and Y. Miyahara, *Sens. Mater.*, **30**, 1175 (2018).